ジ内に残っているすべての空気を注射針を通して外に押し出す。少量の液滴がこぼれても問題ない。**注射針に再びキャップをしないこと。**シリンジを横たえたり，平面に接触させてはならない。

ニューメガの注射

1. 上肢（大腿部），腹部，臀部または上腕部（自己注射しない場合）の皮膚にニューメガを注射することができる［図を参照］。ニューメガを注射するときはそのつど，これらの場所の一つに注射すること。

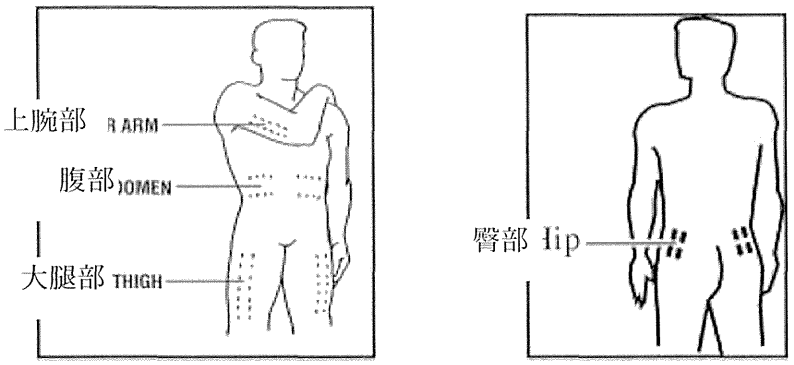

2. 自己注射する場所を決めたら，空いている方の手を使って，アルコールワイプで注射部位の皮膚を消毒する。

3. ニューメガ溶液を含む 1 mL（1 cc）シリンジを用意する。注射針とシリンジの取り付け部分の真上を親指と人さし指でダーツを持つ要領で持ち，シリンジを保持する。もう一方の手の親指と人さし指で，皮膚をつまむ。皮膚をつまんで持ち上げた部分が，ニューメガを注射する場所である。皮膚表面に対し 45°の角度で，皮膚に注射針を穿刺する［図を参照］。一方の手でつまんだ皮膚からそっと手を放し，もう一方の手で皮膚に穿刺した注射針を保持する。

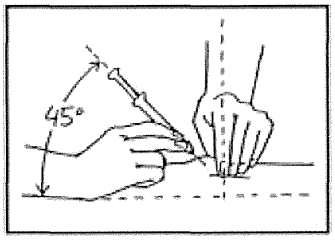

4. 空いている方の手で**そっと**ピストンを後ろに引く。シリンジ内に血液が逆流する場合には，ニューメガを注射しないこと。このような状態になったら，シリンジに取り付けた注射針を皮膚から抜き，本項の手順 7で後述するように，この注射針およびシリンジを耐穿刺性の容器内に廃棄する。ニューメガの新しいボトル，注射用滅菌水（米国薬局方）があらかじめ充填された新しいプレフィルドシリンジ，新しい 1 mL（1 cc）シリンジ，新しい注射針を用いて，前述したすべての手順を繰り返す必要がある。別の部位にニューメガを注射すること。

5. ピストンを後ろに引いたときに，シリンジ内に血液が逆流しなければ，ピストンをゆっくりと最後まで押しきってニューメガを注射する。

6. 注射針の近くに綿ボールをあてて，皮膚から注射針を引き抜く。注射した部位に 3～5 秒間，綿ボー

ルを押しあてておく。**注射した部位を擦らないこと。**

7. **注射針に再びキャップをしないこと。**シリンジを注射針とともに耐穿刺性の容器（“シャープスコンテナー”）内に廃棄する。“シャープスコンテナー”とは，担当医または薬剤師があなたに提供した特殊な箱または容器のことを指す。

   シャープスコンテナーは常に，小児の手の届かないところに置くこと。

   一杯になった容器を適切に処分する方法については，担当医，看護師または薬剤師の指示を受けること。使用済みの注射針およびシリンジの廃棄に関する特別な州法および地域の条例が制定されていることがある。

シャープスコンテナーを家庭ごみとして処分しないこと。また，再利用しないこと。

ニューメガの保存方法

ニューメガ粉末製剤のボトルおよびプレフィルドシリンジを含むキットを冷蔵庫に保存すること。**凍結しないこと。**ニューメガ粉末製剤は，遮光して保存しなければならない。

ニューメガを自己投与するときはそのつど，ニューメガ粉末製剤の新しいボトルと注射用滅菌水（米国薬局方）があらかじめ充填された新しいプレフィルドシリンジを使用しなければならない。ニューメガ粉末製剤のボトルとプレフィルドシリンジには有効期限が印刷されている。有効期限（年月）の過ぎたニューメガまたはプレフィルドシリンジは使用しないこと。

ニューメガ粉末製剤と注射用滅菌水（米国薬局方）を混合・溶解後は，できるだけ速やかに使用しなければならない。ニューメガと注射用滅菌水（米国薬局方）を混合・溶解してから，この溶液を使用するまでに 3 時間以上経過してはならない。ニューメガと注射用滅菌水（米国薬局方）の混合溶液は，ニューメガのボトルに入れたままで室温または冷蔵庫内で3時間まで保存可能である。ボトルを確実に遮光して保存すること。**ニューメガと注射用滅菌水（米国薬局方）の混合溶液をシリンジ内に保存してはならない。**

ニューメガを自己注射した後は，ニューメガのボトルおよび注射針を取り付けたシリンジを“シャープスコンテナー”内に廃棄すること。

シャープスコンテナーを家庭ごみとして処分しないこと。また，再利用しないこと。

処方箋薬についての一般的助言

本薬は，本書に記載されている以外の目的で処方されることもある。ニューメガについて，何らかの疑問点または懸念がある場合には，担当医に相談すること。処方された以外の疾患または処方された患者以外の人に，ニューメガを使用しないこと。

本製品の表示ラベルは，更新されていることがある。本製品の最新の添付文書および詳しい情報については，www.wyeth.com にアクセスするか，当社のメディカルコミュニケーション部門（フリーダイヤル：1-800-934-5556）まで問い合わせること。

Wyeth®

Wyeth Pharmaceuticals Inc.
Philadelphia, PA 19101

US Govt. License No. 3

W10439C011
ET01
Rev 03/09

学 会 等 発 表 実 績

委託業務題目「急性心筋梗塞に対するヒト IL-11 製剤を用いた心筋保護治療の安全性・有効性に関する臨床試験」

機関名　大阪市立大学　大学院医学研究科

１．学会等における口頭・ポスター発表

発表した成果（発表題目、口頭・ポスター発表の別）	発表者氏名	発表した場所（学会等名）	発表した時期	国内・外の別
A nitric oxide synthase inhibitor accelerates high fat diet-induced arteriosclerosis in extremely small size minipig, Microminipig. （ポスター）	Izumi Y, Yamaguchi T, Yamazaki T, Kawaguchi H, Tawa M, Shiota M, Tanimoto A, Okamura T, Yoshiyama M, Iwao H.	京都（第 18 回国際血管生物学会）	2014 年 4 月	国内
Clinical Impact of Drug Therapy Optimization for Heart Failure Using Remote Monitoring in Patients with Cardiac Implantable Electrical Devices. （ポスター）	Takagi M, Sakamoto S, Tatsumi H, Tazawa S, Doi A, Yoshiyama M.	San Francisco, USA (Heart Rhythm Society 2014)	2014 年 5 月	国外
Risk Stratification in Brugada Syndrome: Analysis of Daily Fluctuations in J Wave in Inferolateral Leads and Signal-averaged Electrocardiogram. （ポスター）	Tatsumi H, Takagi M, Sakamoto S, Doi A, Yoshiyama M.	San Francisco, USA (Heart Rhythm Society 2014)	2014 年 5 月	国外
Utility of Combination of T-wave-alternans and Heart rate variability for risk stratification in Brugada syndrome. （ポスター）	Sakamoto S, Takagi M, Tatsumi H, Doi A, Yoshiyama M.	San Francisco, USA (Heart Rhythm Society 2014)	2014 年 5 月	国外
The role of macrophage-derived exosomes in hypertension. （口頭）	Yamaguchi T, Iwao H, Osada-Oka M, Shiota M, Tanaka M, Miura K, Yoshiyama M, Izumi Y.	Athens, Greece (Society of Hypertension/ International Society of Hypertension 2014)	2014 年 6 月	国外
Overexpression of VEGF accelerates right ventricular remodeling due to hypoxia in pulmonary arterial hypertension (PAH) model rats. （ポスター）	Nomura A, Tagawa A, Yamaguchi T, Izumi Y, Yoshiyama M, Sen Y, Fujiwara Y, Matsui M, Kato R, Hayashi T.	Athens, Greece (Society of Hypertension/ International Society of Hypertension 2014)	2014 年 6 月	国外

フレーバーティにおける血管アンチエイジング効果（ポスター）	前田久美子，島田健永，川崎俊博，宮花礼子，上原久美子，豊島範子，河野靖，久保知一郎，田口晴之，葭稔，吉川純一	大阪（日本抗加齢医学会総会）	2014年6月	国内
Risk Stratification in Brugada Syndrome by Using the Combination of T-wave-alternans and Heart Rate Variability.（ポスター）	Sakamoto S, Takagi M, Tatsumi H, Doi A, Yoshiyama M.	東京（日本心電図学会学術集会）	2014年6月	国内
間歇的低酸素負荷がBio14.6心筋症ハムスターの心筋組織病変に与える影響（ポスター）	銭瑶子，野村篤生，加藤隆児，安田侑紀，藤原祐治，松井美佳，室谷美咲，川上淳，井尻好雄，山口雄大，泉康雄，葭山稔，阪本英二，田中一彦，林哲也	福岡（日本循環制御医学会総会）	2014年7月	国内
低酸素負荷におけるO-GlcNAc化タンパク質のオートファジーとアポトーシスへの影響（ポスター）	渡辺明，佐々木泉帆，古川裕一，野村篤生，上和佳，加藤隆児，井尻好雄，中孝俊，山口雄大，泉康雄，葭山稔，朝日通雄，林哲也	福岡（日本循環制御医学会総会）	2014年7月	国内
虚血性心疾患患者の血中バイオマーカーにおける酸化・抗酸化バランス　血漿中ミエロペルオキシダーゼ(MPO)値と血清パラオキソナーゼ-1(PON-1)値の関連（ポスター）	柚木佳，成子隆彦，吉山智貴，杉岡憲一，仲川将志，小松龍士，稲葉真由美，土師一夫，葭山稔，上田真喜子	東京（日本動脈硬化学会総会）	2014年7月	国内
内皮機能検査「FMD」の最新の知見 balMTとFMD　どう使う?　血管機能評価と血管形態評価（口頭）	竹本恭彦，井口朋和，則岡直樹，首藤太一，葭山稔	東京（日本動脈硬化学会総会）	2014年7月	国内
Athological and Immunohistochcmical Findings at Sites of Restenosis and Late Stent Thrombosis after Drug-Eluting Stents.（ポスター）	Masashi N, Naruko T, Sugioka K, Inaba M, Miyazawa T, Kamihata H, Takanashi S, Yoshiyama M, Ueda M.	東京（日本動脈硬化学会総会）	2014年7月	国内
Aortic Arch Calcification on chest X-ray is a simple predictor of Aortic Arch Complex Plaques in patients with Nonvalvular Atrial Fibrillation.（ポスター）	Ito A, Sugioka K, Fujita S, Iwata S, Matsumura Y, Naruko T, Ueda M, Yoshiyama M.	東京（日本動脈硬化学会総会）	2014年7月	国内
Relationship between CHADS2 score and complex aortic plaques by transesophageal echocardiography in patients with nonvalvular atrial fibrillation.（ポスター）	Fujita S, Sugioka K, Iwata S, Matsumura Y, Nakagawa M, Doi A, Takagi M, Ueda M, Yoshiyama M.	東京（日本動脈硬化学会総会）	2014年7月	国内

Serum Levels of High-density Lipoprotein-Associated Paraoxonase-1 Predict Recurrent Cardiovascular Events after Drug-Eluting Stent Implantation in Patients with Stable Angina Pectoris. (ポスター)	Yoshiyama T, Yunoki K, Komatsu R, Haze K, Naruko T, Sugioka K, Nakagawa M, Yoshiyama M, Inaba M, Ueda M.	東京(日本動脈硬化学会総会)	2014年7月	国内
Long-term results of endovascular therapy for below-the-knee lesions in patients with critical limb ischemia in our institution. (ポスター)	Matsuo M, Nishioka H, Katayama H, Kakihara J, Koga Y, Fujimoto K, Kasayuki N, Shimada K, Yoshiyama M.	愛知(日本心血管インターベンション治療学会)	2014年7月	国内
Histlogical findings of Fibromuscular dysplasia in Optical Coherance Tomography. (ポスター)	Mizutani K, Itoh A, Yunoki K, Komatsu R, Haze K, Naruko T, Yoshiyama M.	愛知(日本心血管インターベンション治療学会)	2014年7月	国内
Exosome-mediated intercellular communication by repetitive remote ischemic conditioning reduces left ventricular remodeling on chronic heart failure. (口頭)	Yamaguchi T, Izumi Y, Yamazaki T, Nakamura Y, Sano S, Hanatani A, Shimada K, Iwao H, Yoshiyama M.	Barcelona, Spain (European Society of Cardiology Scientific Session 2014)	2014年8月	国外
Intermittent hypoxia relevant to sleep apnea increases oxidative stress and accelerates systolic dysfunction in heart failure. (ポスター)	Nomura A, Kato R, Sakamoto A, Ijiri Y, Yamaguchi T, Izumi Y, Yoshiyama M, Tanaka K, Hayashi T.	Barcelona, Spain (European Society of Cardiology Scientific Session 2014)	2014年8月	国外
Repetitive treatment of percutaneous carbon dioxide mist prevents high fat diet-induced arteriosclerosis in extremely small size minipig. (ポスター)	Izumi Y, Yamaguchi T, Kawaguchi H, Tawa M, Yamazaki T, Shiota M, Tanimoto A, Okamura T, Yoshiyama M, Iwao H.	Barcelona, Spain (European Society of Cardiology Scientific Session 2014)	2014年8月	国外
Macrophage-derived exosomes damage endothelial cells in experimental hypertensive models. (ポスター)	Izumi Y, Yamaguchi T, Osada-Oka M, Shiota M, Tanaka M, Sano S, Yoshiyama M, Iwao H.	Barcelona, Spain (European Society of Cardiology Scientific Session 2014)	2014年8月	国外
Long-term follow up results of balloon angioplasty for focal renal artery stenosis in young female patients with renovascular hypertension. (ポスター)	Mizutani K, Itoh A, Yunoki K, Komatsu R, Naruko T, Yoshiyama M.	Barcelona, Spain (European Society of Cardiology Scientific Session 2014)	2014年8月	国外

Vascular functional and morphological alterations in smokers with varenicline therap. (ポスター)	Kobayashi M, Takemoto Y, Norioka N, Suto T, Yoshiyama M.	Barcelona, Spain (European Society of Cardiology Scientific Session 2014)	2014年8月	国外
HFpEF患者の予後予測における好感度トロポニンの有用性 (口頭)	Hanatani A, Iwata S, Matsumura Y, Sugioka K, Ehara S, Shimada K, Yoshiyama M.	大阪 (日本心不全学会)	2014年10月	国内
The role of exosomes on cardiac hypertrophy. (ポスター)	Yamaguchi T, Izumi Y, Yamazaki T, Yoshiyama M.	大阪 (日本心不全学会)	2014年10月	国内
Role of o-linked N-acetyl glucosamine posttranslational modification in intermittent hypoxia-induced cardiac remodeling. (ポスター)	Sasaki M, Nakagawa T, Nomura A, Kato R, Ijiri Y, Yamaguchi T, Izumi Y, Yoshiyama M, Asahi M, Hayashi T.	大阪 (日本心不全学会)	2014年10月	国内
Intermittent hypoxia Relevant to sleep apnea increases oxidative stress and accelerates cardiac remodeling in cardiomyopathic hamster. (ポスター)	Muroya M, Nomura A, Kato R, Ijiri Y, Sakamoto A, Yamaguchi T, Izumi Y, Yoshiyama M, Tanaka K, Hayashi T.	大阪 (日本心不全学会)	2014年10月	国内
VEGF overexpression and right ventricular remodeling in rats exposed to chronic hypoxia. (ポスター)	Matsui M, Woo E, Katsumata T, Yamaguchi T, Yoshiyama M, Izumi Y, Nomura A, Fujiwara Y, Kato R, Hayashi T.	大阪 (日本心不全学会)	2014年10月	国内
超小型ミニブタを用いたメタボリック症候群モデル作製 (ポスター)	泉康雄, 山崎貴紀, 中村泰浩, 島田健永, 葭山稔, 岩尾洋	神奈川(日本高血圧学会)	2014年10月	国内
Visit-to-Visit 平均透析中血圧高値は透析患者の大動脈弁狭窄症進行促進因子である (口頭)	則岡直樹, 岩田真一, 柳志郎, 八木秀也, 吉田啓子, 蒔田直記, 白井たから, 石井英, 紙森公雄, 太田剛弘, 葭山稔	神奈川(日本高血圧学会)	2014年10月	国内
若年健康女性医療従事者における夜勤が夜間血圧に与える影響 (口頭)	北田諒子, 岩田真一, 花谷彰久, 杉岡憲一, 葭山稔	神奈川(日本高血圧学会)	2014年10月	国内

2．学会誌・雑誌等における論文掲載

掲載した論文 (発表題目)	発表者氏名	発表した場所 (学会誌・雑誌等名)	発表した時期	国内・外の別
Serum n-3 to n-6 polyunsaturated fatty acids ratio correlates with coronary plaque vulnerability: an optical coherence tomography study.	Hasegawa T, Otsuka K, Iguchi T, Matsumoto K, Ehara S, Nakata S, Nishimura S, Kataoka T, Shimada K, Yoshiyama M.	Heart Vessels	2014年	国外

The strain pattern, and not Sokolow-Lyon electrocardiographic voltage criteria, is independently associated with anatomic left ventricular hypertrophy.	Ehara S, Hasegawa T, Matsumoto K, Otsuka K, Yamazaki T, Iguchi T, Izumi Y, Shimada K, Yoshiyama M.	Heart Vessels	2014年	国外
Prognosis of vulnerable plaque on computed tomographic coronary angiography with normal myocardial perfusion image.	Otsuka K, Fukuda S, Tanaka A, Nakanishi K, Taguchi H, Yoshiyama M, Shimada K, Yoshikawa J.	Eur Heart J Cardiovasc Imaging	2014年	国外
Giant mycotic coronary aneurysm associated with late stent infection.	Nonin S, Hasegawa T, Hirai H, Suehiro S, Yoshiyama M.	Eur Heart J Cardiovasc Imaging	2014年	国外
Insulin resistance is associated with coronary plaque vulnerability: insight from optical coherence tomography analysis.	Iguchi T, Hasegawa T, Otsuka K, Matsumoto K, Yamazaki T, Nishimura S, Nakata S, Ehara S, Kataoka T, Shimada K, Yoshiyama M.	Eur Heart J Cardiovasc Imaging	2014年	国外
Lipid synthesis is promoted by hypoxic adipocyte-derived exosomes in 3T3-L1 cells.	Sano S, Izumi Y, Yamaguchi T, Yamazaki T, Tanaka M, Shiota M, Osada-Oka M, Nakamura Y, Wei M, Wanibuchi H, Iwao H, Yoshiyama M.	Biochem Biophys Res Commun	2014年	国外
Enhanced expression of hemoglobin scavenger receptor and heme oxygenase-1 is associated with aortic valve stenosis in patients undergoing hemodialysis.	Inaba M, Sugioka K, Naruko T, Yunoki K, Kato Y, Shibata T, Inoue T, Ohsawa M, Yoshiyama M, Ueda M.	Hemodial Int	2014年	国外
Chronic active Epstein-Barr virus infection complicated with multiple artery aneurysms.	Nishimura S, Ehara S, Hanatani A, Yoshiyama M.	Eur Heart J Cardiovasc Imaging	2014年	国外
Serial assessment of arterial stiffness by cardio-ankle vascular index for prediction of future cardiovascular events in patients with coronary artery disease.	Otsuka K, Fukuda S, Shimada K, Suzuki K, Nakanishi K, Yoshiyama M, Yoshikawa J.	Hypertens Res	2014年	国内
Relationship between CHADS2 score and complex aortic plaques by transesophageal echocardiography in patients with nonvalvular atrial fibrillation.	Sugioka K, Fujita S, Iwata S, Ito A, Matsumura Y, Hanatani A, Doi A, Takagi M, Naruko T, Ueda M, Yoshiyama M.	Ultrasound Med Biol	2014年	国外

A noninvasive metabolic syndrome model using an extremely small minipig, the microminipig.	Yamaguchi T, Yamazaki T, Kawaguchi H, Tawa M, Nakamura Y, Shiota M, Osada-Oka M, Tanimoto A, Okamura T, Miura K, Iwao H, Yoshiyama M, Izumi Y.	J Pharmacol Sci	2014年	国内
Differences between rosuvastatin and atorvastatin in lipid-lowering action and effect on glucose metabolism in Japanese hypercholesterolemic patients with concurrent diabetes. Lipid-lowering with highly potent statins in hyperlipidemia with type 2 diabetes patients (LISTEN) study.	Ogawa H, Matsui K, Saito Y, Sugiyama S, Jinnouchi H, Sugawara M, Masuda I, Mori H, Waki M, Yoshiyama M, Watada H.	Circ J	2014年	国内
Hydrogen gas attenuates embryonic gene expression and prevents left ventricular remodeling induced by intermittent hypoxia in cardiomyopathic hamsters.	Kato R, Nomura A, Sakamoto A, Yasuda Y, Amatani K, Nagai S, Sen Y, Ijiri Y, Okada Y, Yamaguchi T, Izumi Y, Yoshiyama M, Tanaka K, Hayashi T.	Am J Physiol Heart Circ Physiol	2014年	国外
Association between chronic kidney disease and thoracic aortic atherosclerosis detected using transesophageal echocardiography.	Matsumura Y, Sugioka K, Fujita S, Ito A, Iwata S, Yoshiyama M.	Atherosclerosis	2014年	国外
Long-term prognostic impact of the attenuated plaque in patients with acute coronary syndrome.	Okura H, Kataoka T, Yoshiyama M, Yoshikawa J, Yoshida K.	Heart Vessels	2015年	国外
Repeated remote ischemic conditioning attenuates left ventricular remodeling via exosome-mediated intercellular communication on chronic heart failure after myocardial infarction.	Yamaguchi T, Izumi Y, Nakamura Y, Yamazaki T, Shiota M, Sano S, Tanaka M, Osada-Oka M, Shimada K, Miura K, Yoshiyama M, Iwao H.	Int J Cardiol	2015年	国外
Percutaneous Carbon Dioxide Treatment using a Gas Mist Generator Enhances the Collateral Blood Flow in the Ischemic Hindlimb.	Izumi Y, Yamaguchi T, Yamazaki T, Yamashita N, Nakamura Y, Shiota M, Tanaka M, Sano S, Osada-Oka M, Shimada K, Wanibuchi H, Miura K, Yoshiyama M, Iwao H.	J Atheroscler Thromb	2015年	国内

Characteristic patterns of the longitudinal and circumferential distribution of calcium deposits by parent coronary arteries observed from computed tomography angiography.	Ehara S, Matsumoto K, Hasegawa T, Otsuka K, Sakaguchi M, Shimada K, Yoshikawa J, Yoshiyama M.	Heart Vessels	2015年	国外

研究成果の主要刊行物・印刷

Heart Vessels (2014) 29:596–602
DOI 10.1007/s00380-013-0404-4

ORIGINAL ARTICLE

Serum n-3 to n-6 polyunsaturated fatty acids ratio correlates with coronary plaque vulnerability: an optical coherence tomography study

Takao Hasegawa · Kenichiro Otsuka · Tomokazu Iguchi · Kenji Matsumoto · Shoichi Ehara · Shinji Nakata · Satoshi Nishimura · Toru Kataoka · Kenei Shimada · Minoru Yoshiyama

Received: 30 April 2013 / Accepted: 16 August 2013 / Published online: 5 September 2013
© Springer Japan 2013

Abstract A low ratio of eicosapentaenoic acid to arachidonic acid (EPA/AA) has been demonstrated to be associated with a higher risk of cardiovascular events. Optical coherence tomography (OCT) is useful for the assessment of coronary plaque vulnerability. The purpose of this study was to evaluate the association between EPA/AA ratio and coronary plaque vulnerability. This study involved 58 patients with stable angina pectoris undergoing percutaneous coronary intervention. OCT image acquisition was performed before the procedure in the culprit lesions. We assessed lipid-rich plaque length and arc, fibrous cap thickness, frequency of thin-cap fibroatheroma (TCFA), thrombus, ruptured plaque, macrophage infiltration, and microvessels using OCT. Patients were divided into two groups according to the median value of serum EPA/AA ratio: a low-EPA/AA group (n = 29, EPA/AA ratio <0.36) and a high-EPA/AA group (n = 29, EPA/AA ratio ≥0.36). In qualitative analyses, TCFA (35.4 vs 6.9 %, P = 0.0095), macrophage infiltration (48.3 vs 13.8 %, P = 0.0045), and microvessels (44.8 vs 10.3 %, P = 0.0033) were more frequently observed in the low-EPA/AA group. In quantitative analyses, the low-EPA/AA group had wider maximum lipid arc (114.0 ± 94.8° vs 56.4 ± 66.0°, P = 0.0097), longer lipid length (4.8 ± 4.5 vs 1.6 ± 2.6 mm, P = 0.0037), and thinner fibrous cap (69.3 ± 28.3 vs 113.3 ± 46.6 μm, P = 0.005) compared with the high-EPA/AA group. EPA/AA ratio was positively correlated with fibrous cap thickness (r = 0.46, P = 0.007). In a multivariate model, an EPA/AA ratio <0.36 was associated with the presence of TCFA (odds ratio 6.41, 95 % confidence interval 1.11–61.91, P = 0.0371). In our detailed OCT analysis, lower EPA/AA ratio was associated with higher vulnerability of coronary plaques to rupture.

Keywords Eicosapentaenoic acid to arachidonic acid ratio · Vulnerable plaque · Optical coherence tomography

Introduction

Intensive lipid-lowering therapy with statins is regarded as one of the effective treatments for the stabilization of coronary artery plaques, and reduces the risk for coronary events and mortality [1–3]. However, cardiovascular events occur in some patients even with statin therapy. Previous studies have shown that consumption of fish and fish oils was associated with a decreased risk of cardiovascular disease. Fish and fish oil are sources of the omega-3 fatty acid eicosapentaenoic acid (EPA). A high serum ratio of EPA to arachidonic acid (AA) may play an important role in preventing future cardiovascular events and contributing to a better outcome [4–6]. The Japan EPA Lipid Intervention Study (JELIS), a large randomized clinical trial, showed that purified EPA administration along with statin therapy reduced the incidence of coronary events by 19 % compared with statin therapy alone [7].

T. Hasegawa (✉) · K. Otsuka · T. Iguchi · K. Matsumoto · S. Ehara · S. Nakata · K. Shimada · M. Yoshiyama
Department of Cardiovascular Medicine, Graduate School of Medicine, Osaka City University, 1-4-3 Asahi-machi, Abeno-ku, Osaka 545-8585, Japan
e-mail: takao0321@aol.com

S. Nishimura
Division of Cardiology, Kawasaki Hospital, Okayama, Japan

T. Kataoka
Division of Cardiology, Bell-Land General Hospital, Osaka, Japan

Atherosclerosis has an important inflammatory component, and acute cardiovascular events can be initiated by inflammatory processes occurring in vulnerable plaques [8–10]. A major cause of acute coronary syndrome (ACS) is the disruption of vulnerable plaques with superimposed thrombus. The anti-inflammatory effects of marine n-3 polyunsaturated fatty acids (PUFAs) may contribute to their protective actions toward atherosclerosis, plaque rupture, and cardiovascular mortality [11]. Optical coherence tomography (OCT) is a high-resolution imaging technology that can provide a detailed observation of the vulnerable coronary plaque, such as thin-cap fibroatheroma (TCFA), plaque rupture, and intracoronary thrombus.

The purpose of this study was to investigate the association between the serum EPA/AA ratio and plaque vulnerability evaluated by OCT.

Patients and methods

Study patients

This study enrolled 312 consecutive patients with ACS or stable angina pectoris who underwent percutaneous coronary intervention (PCI) and an intracoronary OCT examination. The exclusion criteria were ACS, congestive heart failure, cardiogenic shock, an intercurrent infection or other inflammatory disease, in-stent restenosis, total occluded lesion, lesions with large quantity of thrombus, no blood samples, and poor image quality of OCT for analysis. According to these exclusion criteria, ultimately 58 patients were enrolled into this study. We divided these patients into two groups according to the median value of serum EPA/AA ratio: patients with a low EPA/AA ratio ($n = 29$, EPA/AA ratio <0.36) and patients with a high EPA/AA ratio ($n = 29$, EPA/AA ratio ≥ 0.36). OCT findings in the culprit lesions were compared between the two groups.

Blood samples were obtained in the fasting state on admission for measurements of PUFAs (EPA, AA, and docosahexaenoic acid (DHA)). The measurement was performed by gas chromatography at the central laboratory (SRL, Tokyo, Japan). In brief, serum lipids were extracted by Folch's procedure, then fatty acids (tricosanoic acid, C23:0, as the internal standard) were methylated with boron trifluoride and methanol. The methylated fatty acids were then analyzed using a gas chromatograph (GC-2010; Shimadzu, Kyoto, Japan) equipped with a capillary column (TC-70; GL Sciences, Tokyo, Japan).

ACS includes acute myocardial infarction defined by The Joint European Society of Cardiology/American College of Cardiology Committee, and unstable angina pectoris defined according to the Braunwald clinical classification. Hypertension was defined by the Joint National Committee VII, diabetes mellitus by the World Health Organization (WHO) Study Group, and hypercholesterolemia by the Japan Atherosclerosis Society Guidelines. The study was approved by the hospital ethics committee, and informed consent was obtained from all patients before the study.

OCT image acquisition and analysis

OCT imaging was performed before PCI and after the administration of 100–200 mg intracoronary nitroglycerin. In the present study, images were acquired using a time-domain (M2CV OCT Imaging System; LightLab Imaging, Westford, MA, USA) or a frequency-domain (C7-XR OCT Intravascular Imaging System; St Jude Medical, St Paul, MN, USA) OCT system. The intracoronary OCT imaging technique has been described previously [12, 13]. In the M2 system, a 0.016-inch OCT catheter was advanced to the culprit lesion through a 3-F occlusion balloon catheter. To remove the blood from the field of view, the occlusion balloon was inflated to 0.6 atm at the proximal site of the culprit lesion, and Lactated Ringer's solution was infused into the coronary artery from the distal tip of the occlusion balloon catheter at 0.5 mL/s. The entire length of the culprit lesion was imaged using an automatic pullback device moving at 1 mm/s, and the OCT image clearly visualized the culprit lesion. In the C7 system, a 2.7-F OCT imaging catheter (Dragonfly; LightLab Imaging, Westford, MA, USA) is advanced distal to the lesion; automatic pullback was started as soon as the blood was cleared by the injection of contrast media or Dextran. All images were stored digitally for subsequent offline analysis.

OCT image analysis was performed by two experienced observers blinded to the clinical information by using previously established criteria for OCT plaque characterization [14]. OCT analysis was performed in the culprit lesion. The presence of TCFA, plaque rupture, macrophage infiltration, microvessels, and intracoronary thrombus were evaluated. When lipid was present in ≥ 2 quadrants in any of the images within a plaque, it was considered a lipid-rich plaque. In the culprit lesion, maximum lipid arc was measured. Lipid length was defined as length of lipid-rich plaque and measured on longitudinal view. TCFA was defined as a lipid-rich plaque with a fibrous cap thickness measuring ≤ 65 μm. The fibrous cap thickness of lipid-rich plaque was measured at the thinnest part three times, and the average value was then calculated. Plaque rupture was defined as an intimal interruption and cavity formation in the plaque. Macrophage infiltration was defined as bright spots with high OCT backscattering signal variances. A microvessel was defined as a no-signal tubular structure without a connection to the vessel lumen recognized on ≥ 3 consecutive cross-sectional images. Thrombus was identified as an

Table 1 Patients' characteristics

	All (n = 58)	Low EPA/AA (n = 29)	High EPA/AA (n = 29)	P value*
Age (years)	69 ± 9	67 ± 9	71 ± 9	0.17
Male, n (%)	39 (67)	19 (66)	20 (69)	0.78
Body mass index (kg/m^2)	24.7 ± 3.4	25.4 ± 2.8	24.0 ± 3.9	0.12
Coronary risk factor, n (%)				
Smoking	35 (60)	16 (55)	19 (66)	0.42
Hypertension	50 (86)	24 (82)	26 (90)	0.45
Diabetes	38 (66)	20 (69)	18 (62)	0.58
Dyslipidemia	44 (76)	22 (76)	22 (76)	1.00
Cardiovascular history, n (%)				
Myocardial infarction	16 (28)	8 (28)	8 (28)	1.00
PTCA or CABG	29 (50)	16 (55)	13 (45)	0.43
Culprit vessel, n (%)				0.18
LAD	28 (48)	15 (52)	13(45)	
LCx	12 (21)	8 (27)	4 (14)	
RCA	18 (31)	6 (21)	12 (41)	
Culprit lesion				
%DS, (%)	67.2 ± 9.9	68.1 ± 10.0	66.3 ± 9.8	0.49
Type B2/C, n (%)	45 (78)	22 (76)	23 (79)	0.75
Medication use, n (%)				
Antiplatelet agent	50 (86)	27 (93)	23 (79)	0.13
β-Blocker	20 (35)	9 (31)	11 (38)	0.58
ACE-I/ARB	33 (57)	15 (52)	18 (62)	0.43
Statin	32 (55)	19 (66)	13 (45)	0.11

EPA/AA eicosapentaenoic acid (EPA) to arachidonic acid (AA) ratio, *PTCA* percutaneous transluminal coronary angioplasty, *CABG* coronary-artery bypass grafting, *LAD* left anterior descending coronary artery, *LCx* left circumflex coronary artery, *RCA* right coronary artery, *%DS* percent diameter stenosis, *ACE-I* angiotensin-converting enzyme inhibitor, *ARB* angiotensin receptor blocker

* P value for low vs high EPA/AA ratio

irregular high- or low-backscattering mass protruding into the lumen. If there was discordance of diagnosis between the two observers, a consensus diagnosis was obtained using repeated off-line readings.

Statistical analysis

Continuous variables were presented as mean ± standard deviation (SD). Comparisons were conducted by Student's t test or nonparametric Wilcoxon sum rank test for non-normally distributed variables. Categorical variables were compared by Chi-square test. Multivariate logistic regression analyses were performed to identify independent predictors of OCT-detected vulnerable findings (TCFA, plaque rupture, macrophage infiltration, microvessels, and thrombus) by adjusting for predefined variables. Low-density lipoprotein (LDL) cholesterol, high-density lipoprotein (HDL) cholesterol, high-sensitivity C-reactive protein (hsCRP), EPA/AA ratio, and DHA were included in the multivariate logistic model. A P value of less than 0.05 was considered statistically significant. Statistical analysis was performed with JMP, version 10 for windows (SAS Institute, Cary, NC, USA).

Results

Table 1 shows the patients' characteristics. The mean age of all patients was 69 years, and 39 patients (67 %) were men. There were no differences in the patient' characteristics between the two groups. EPA and EPA/AA ratio were significantly lower in low-EPA/AA group than in the high-EPA/AA group. There were no differences in the serum lipid profile (total cholesterol, LDL cholesterol, HDL cholesterol, and triglycerides) between the two groups. There was no significant difference in hsCRP between the low- and high-EPA/AA groups (0.36 ± 1.24 vs 0.23 ± 0.33, P = 0.58) (Table 2).

The comparison of plaque characteristics by OCT in the low- and high-EPA/AA groups is shown in Table 3. The representative OCT images of the coronary culprit lesions in the low and high-EPA/AA groups are shown in Figs. 1

Table 2 Serum lipid profile and fatty acid composition in low- and high-EPA/AA groups

	Low EPA/AA (n = 29)	High EPA/AA (n = 29)	P value
Serum lipid value, mg/dl			
Total cholesterol	175.8 ± 35.3	175.8 ± 38.0	0.99
LDL cholesterol	101.4 ± 35.4	100.3 ± 29.6	0.90
HDL cholesterol	39.8 ± 12.6	43.1 ± 13.3	0.25
Triglycerides	148.8 ± 75.3	139.7 ± 89.6	0.42
PUFA value, μg/ml			
EPA	47.2 ± 14.5	90.5 ± 36.4	<0.0001
AA	190.2 ± 53.0	160.8 ± 48.4	0.03
DHA	136.1 ± 36.1	164.8 ± 52.7	0.02
EPA/AA ratio	0.26 ± 0.07	0.59 ± 0.26	<0.0001

EPA/AA eicosapentaenoic acid (EPA) to arachidonic acid (AA) ratio, *LDL* low-density lipoprotein, *HDL* high-density lipoprotein, *PUFA* polyunsaturated fatty acid, *DHA* docosahexaenoic acid

Table 3 Plaque characteristics of optical coherence tomography in low- and high-EPA/AA groups

	Low EPA/AA (n = 29)	High EPA/AA (n = 29)	P value
Minimal CSA, mm^2	1.4 ± 0.8	1.6 ± 0.8	0.26
Lipid-rich plaque, n (%)	14 (48.3)	8 (27.6)	0.10
Maximum lipid arc, (°)	114.0 ± 94.8	56.4 ± 66.0	0.0097
Lipid length, mm	4.8 ± 4.5	1.6 ± 2.6	0.0037
TCFA, n (%)	10 (34.5)	2 (6.9)	0.0095
Fibrous cap thickness, μm	69.3 ± 28.3	113.3 ± 46.6	0.005
Plaque rupture, n (%)	5 (17.2)	1 (3.5)	0.08
Macrophage infiltration, n (%)	14 (48.3)	4 (13.8)	0.0045
Microvessels, n (%)	13 (44.8)	3 (10.3)	0.0033
Thrombus, n (%)	6 (20.7)	4 (13.8)	0.49

EPA/AA eicosapentaenoic acid (EPA) to arachidonic acid (AA) ratio, *CSA* cross-sectional area, *TCFA* thin-cap fibroatheroma

and 2. According to qualitative analysis, TCFA (35.4 vs 6.9 %, $P = 0.0095$), macrophages (48.3 vs 13.8 %, $P = 0.0045$), and microvessels (44.8 vs 10.3 %, $P = 0.0033$) were more frequently observed in the low-EPA/AA group. The frequency of plaque rupture tended to be higher in the low-EPA/AA group (17.2 vs 3.5 %, $P = 0.08$). There were no significant differences in the presence of lipid-rich plaque and thrombus. According to quantitative analysis, the low-EPA/AA group had a wider maximum lipid arc compared with the high-EPA/AA group (114.0 ± 94.8° vs 56.4 ± 66.0°, $P = 0.0097$), longer lipid length (4.8 ± 4.5 vs 1.6 ± 2.6 mm, $P = 0.0037$), and thinner fibrous cap (69.3 ± 28.3 vs 113.3 ± 46.6 μm, $P = 0.005$). The EPA/AA ratio was positively correlated with fibrous cap thickness ($r = 0.46$, $P = 0.007$) (Fig. 2).

In the multivariate logistic regression model including LDL cholesterol, HDL cholesterol, hsCRP, EPA/AA ratio, and DHA, an EPA/AA ratio <0.36 had a significant association with the presence of TCFA (odds ratio 6.41, 95 % confidence interval 1.11–61.91, $P = 0.0371$).

Discussion

The present study showed that the EPA/AA ratio was associated with coronary plaque vulnerability of the culprit lesions by OCT examination in patients with stable angina pectoris. A low EPA/AA ratio had significant association with a thinner fibrous cap, larger lipid-arc length, and higher prevalence of TCFA, macrophages, and microvessels. An EPA/AA ratio <0.36 was a predictor for the presence of TCFA. The EPA/AA ratio was positively correlated with fibrous cap thickness.

Epidemiologic and clinical evidence suggests that an increased intake of marine n-3 PUFAs has protective effects against the cardiovascular events and mortality, including sudden cardiac death [7, 15, 16]. Inflammation is now recognized to play an important role in atherosclerosis [17, 18]. The anti-inflammatory actions of marine n-3 PUFAs may stabilize atherosclerotic plaques by decreasing infiltration of inflammatory and immune cells into the plaques, and by decreasing the activity of those cells once in the plaque [11]. Our study demonstrated that macrophage infiltration was lower in the high-EPA/AA group, which could offer one of the explanations for that mechanism. The protective effects of marine n-3 PUFAs against atherosclerosis have been confirmed in previous animal and human studies [19, 20]. In the animal study, Apolipoprotein E-deficient or low-density lipoprotein receptor-deficient mice were fed a Western-type diet or the same diet plus EPA for 12 weeks. EPA reduced aortic lipid deposition, consistent with earlier animal studies. EPA

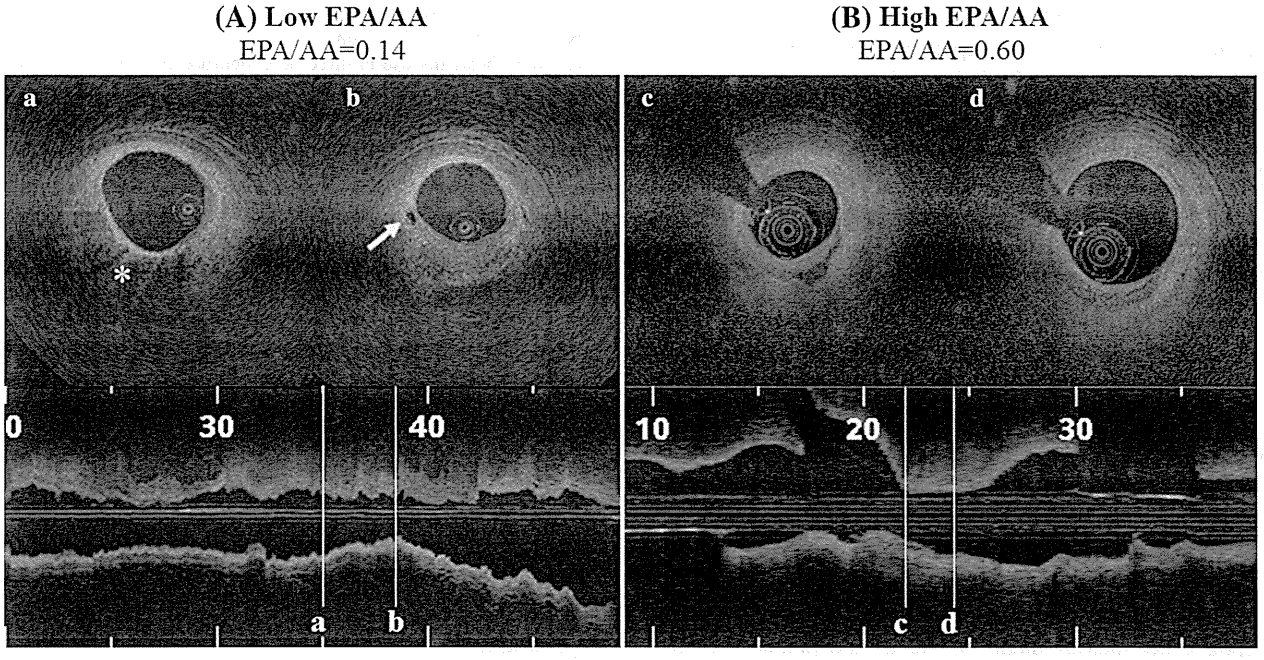

Fig. 1 Representative optical coherence tomography (OCT) images of the culprit lesions. The *left* (**A**) and *right figures* (**B**) are representative OCT images of low- and high-EPA/AA groups, respectively. In the case of the low-EPA/AA group, OCT cross-sectional images show thin-cap fibroatheroma (thickness of the fibrous cap = 63 μm) with macrophage infiltration (*asterisk*) from the 6 o'clock to the 9 o'clock position (**a**) and a microvessel (*arrow*) observed as black holes within a plaque in the 9 o'clock position (**b**). In the case of the low-EPA/AA group, fibrocalcified plaques were observed (**c**, **d**). *EPA/AA* eicosapentaenoic acid to arachidonic acid ratio

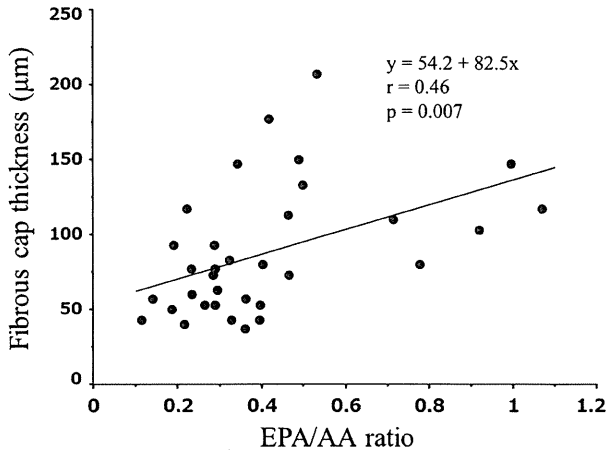

Fig. 2 Correlation between fibrous cap thickness and EPA/AA ratio. There was significant correlation between EPA/AA ratio and fibrous cap thickness identified by optical coherence tomography (r = 0.46, P = 0.007). *EPA/AA* eicosapentaenoic acid to arachidonic acid ratio

resulted in increased plaque collagen and decreased macrophage numbers in the plaque. The human intervention study conducted in patients awaiting carotid endarterectomy showed that marine n-3 fatty acids are incorporated from dietary fish-oil supplements into advanced atherosclerotic plaques, and that this incorporation is associated with structural changes consistent with increased plaque stability including reduced macrophage infiltration. In the present study, coronary plaque vulnerability by OCT was higher in the low-EPA/AA group than in the high-EPA/AA group.

The current understanding of the major cause of ACS is that it results from rupture of a vulnerable plaque [21, 22]. OCT is a high-resolution imaging technology, which can provide detailed observation of the vulnerable coronary plaque. TCFA is recognized as a precursor lesion for plaque rupture. In the present study, multivariate analysis adjusted for LDL cholesterol, HDL cholesterol, hsCRP, EPA/AA ratio, and DHA revealed that a lower EPA/AA ratio (EPA/AA ratio <0.36) was an independent factor for predicting the presence of TCFA. Moreover, the EPA/AA ratio was positively correlated with fibrous cap thickness. Inflammatory cytokine production and expression of adhesion molecules play important roles in the activation of macrophage foam cells, resulting in plaque development and weakening of fibrous cap [8, 23]. n-3 PUFAs have protective effects against coronary plaque vulnerability by inhibiting inflammatory cytokine production and expression of adhesion molecules [24, 25]. These mechanisms might support our results.

To our knowledge, the present study is the first to examine the association between EPA/AA ratios and coronary plaque

vulnerability in patients with stable angina pectoris by OCT. On the basis of a previous report, the results of which are consistent our own, the EPA/AA ratio affects the coronary plaque vulnerability of nonculprit lesions in patients with stable angina pectoris [26]. Even with aggressive statin therapy, a high residual risk of cardiovascular events remains, and draws attention to the need for additional preventive therapies [27, 28]. Additional treatment with n-3 PUFAs in combination with statin therapy may be a therapeutic approach to preventing future cardiovascular events, because increases in serum EPA to AA ratios are associated with low coronary plaque vulnerability.

Study limitations

This study had several limitations. First, the number of subjects included was too small for evaluation of contributing factors to the findings of vulnerable coronary plaque by OCT. Second, owing to the limited axial penetration depth, exact measurements of vessel and plaque area by OCT were not possible. Third, plaque rupture, microvessels, macrophages, and thrombus were only used for qualitative analysis and were not strictly validated. Fourth, images were acquired using two kinds of OCT imaging systems: time-domain or frequency-domain OCT. Fifth, we did not perform OCT analyses in all three coronary vessels.

Conclusions

A lower EPA/AA ratio was associated with higher vulnerability of coronary plaques. Purified EPA administration may have protective effects against vulnerable coronary plaque.

Conflict of interest There are no conflicts of interest to disclose in connection with any commercial associations for any of the authors.

References

1. Deedwania P, Stone PH, Bairey Merz CN, Cosin-Aguilar J, Koylan N, Luo D, Ouyang P, Piotrowicz R, Schenck-Gustafsson K, Sellier P, Stein JH, Thompson PL, Tzivoni D (2007) Effects of intensive versus moderate lipid-lowering therapy on myocardial ischemia in older patients with coronary heart disease: results of the Study Assessing Goals in the Elderly (SAGE). Circulation 115:700–707
2. LaRosa JC, Grundy SM, Waters DD, Shear C, Barter P, Fruchart JC, Gotto AM, Greten H, Kastelein JJ, Shepherd J, Wenger NK, Treating to New Targets Investigators (2005) Intensive lipid lowering with atorvastatin in patients with stable coronary disease. N Engl J Med 352:1425–1435
3. Lauderdale SA, Sheehan AH (2005) Intensive lipid-lowering therapy in patients with coronary heart disease. Ann Pharmacother 39:329–334
4. Nakamura T, Azuma A, Kuribayashi T, Sugihara H, Okuda S, Nakagawa M (2003) Serum fatty acid levels, dietary style and coronary heart disease in three neighbouring areas in Japan: the Kumihama study. Br J Nutr 89:267–272
5. Domei T, Yokoi H, Kuramitsu S, Soga Y, Arita T, Ando K, Shirai S, Kondo K, Sakai K, Goya M, Iwabuchi M, Ueeda M, Nobuyoshi M (2012) Ratio of serum n-3 to n-6 polyunsaturated fatty acids and the incidence of major adverse cardiac events in patients undergoing percutaneous coronary intervention. Circ J 76:423–429
6. Ueeda M, Doumei T, Takaya Y, Ohnishi N, Takaishi A, Hirohata S, Miyoshi T, Shinohata R, Usui S, Kusachi S (2011) Association of serum levels of arachidonic acid and eicosapentaenoic acid with prevalence of major adverse cardiac events after acute myocardial infarction. Heart Vessels 26:145–152
7. Yokoyama M, Origasa H, Matsuzaki M, Matsuzawa Y, Saito Y, Ishikawa Y, Oikawa S, Sasaki J, Hishida H, Itakura H, Kita T, Kitabatake A, Nakaya N, Sakata T, Shimada K, Shirato K (2007) Effects of eicosapentaenoic acid on major coronary events in hypercholesterolaemic patients (JELIS): a randomised open-label, blinded endpoint analysis. Lancet 369:1090–1098
8. Hansson GK (2005) Inflammation, atherosclerosis, and coronary artery disease. N Engl J Med 352:1685–1695
9. Stoll G, Bendszus M (2006) Inflammation and atherosclerosis: novel insights into plaque formation and destabilization. Stroke 37:1923–1932
10. Libby P (2012) Inflammation in atherosclerosis. Arterioscler Thromb Vasc Biol 32:2045–2051
11. Calder PC (2012) The role of marine omega-3 (n-3) fatty acids in inflammatory processes, atherosclerosis and plaque stability. Mol Nutr Food Res 56:1073–1080
12. Onuma Y, Serruys PW, Perkins LE, Okamura T, Gonzalo N, Garcia–Garcia HM, Regar E, Kamberi M, Powers JC, Rapoza R, van Beusekom H, van der Giessen W, Virmani R (2010) Intracoronary optical coherence tomography and histology at 1 month and 2, 3, and 4 years after implantation of everolimus-eluting bioresorbable vascular scaffolds in a porcine coronary artery model: an attempt to decipher the human optical coherence tomography images in the ABSORB trial. Circulation 122:2288–2300
13. Takarada S, Imanishi T, Liu Y, Ikejima H, Tsujioka H, Kuroi A, Ishibashi K, Komukai K, Tanimoto T, Ino Y, Kitabata H, Kubo T, Nakamura N, Hirata K, Tanaka A, Mizukoshi M, Akasaka T (2010) Advantage of next-generation frequency-domain optical coherence tomography compared with conventional time-domain system in the assessment of coronary lesion. Catheter Cardiovasc Interv 75:202–206
14. Tearney GJ, Regar E, Akasaka T, Adriaenssens T, Barlis P, Bezerra HG, Bouma B, Bruining N, Cho JM, Chowdhary S, Costa MA, de Silva R, Dijkstra J, Di Mario C, Dudek D, Falk E, Feldman MD, Fitzgerald P, Garcia-Garcia HM, Gonzalo N, Granada JF, Guagliumi G, Holm NR, Honda Y, Ikeno F, Kawasaki M, Kochman J, Koltowski L, Kubo T, Kume T, Kyono H, Lam CC, Lamouche G, Lee DP, Leon MB, Maehara A, Manfrini O, Mintz GS, Mizuno K, Morel MA, Nadkarni S, Okura H, Otake H, Pietrasik A, Prati F, Raber L, Radu MD, Rieber J, Riga M, Rollins A, Rosenberg M, Sirbu V, Serruys PW, Shimada K, Shinke T, Shite J, Siegel E, Sonoda S, Suter M, Takarada S, Tanaka A, Terashima M, Thim T, Uemura S, Ughi GJ, van Beusekom HM, van der Steen AF, van Es GA, van Soest G, Virmani R, Waxman S, Weissman NJ, Weisz G, International Working Group for Intravascular Optical Coherence Tomography (2012) Consensus standards for acquisition, measurement, and reporting of intravascular optical coherence tomography studies: a report from the International Working Group for Intravascular Optical Coherence Tomography Standardization and Validation. J Am Coll Cardiol 59:1058–1072

15. Gruppo Italiano per lo Studio della Sopravvivenza nell'Infarto miocardico (1999) Dietary supplementation with n-3 polyunsaturated fatty acids and vitamin E after myocardial infarction: results of the GISSI-Prevenzione trial. Lancet 354:447–455
16. Albert CM, Campos H, Stampfer MJ, Ridker PM, Manson JE, Willett WC, Ma J (2002) Blood levels of long-chain n-3 fatty acids and the risk of sudden death. N Engl J Med 346:1113–1118
17. van der Wal AC, Becker AE, van der Loos CM, Das PK (1994) Site of intimal rupture or erosion of thrombosed coronary atherosclerotic plaques is characterized by an inflammatory process irrespective of the dominant plaque morphology. Circulation 89:36–44
18. Bogaty P, Poirier P, Simard S, Boyer L, Solymoss S, Dagenais GR (2001) Biological profiles in subjects with recurrent acute coronary events compared with subjects with long-standing stable angina. Circulation 103:3062–3068
19. Matsumoto M, Sata M, Fukuda D, Tanaka K, Soma M, Hirata Y, Nagai R (2008) Orally administered eicosapentaenoic acid reduces and stabilizes atherosclerotic lesions in ApoE-deficient mice. Atherosclerosis 197:524–533
20. Thies F, Garry JM, Yaqoob P, Rerkasem K, Williams J, Shearman CP, Gallagher PJ, Calder PC, Grimble RF (2003) Association of n-3 polyunsaturated fatty acids with stability of atherosclerotic plaques: a randomised controlled trial. Lancet 361:477–485
21. Virmani R (2011) Are our tools for the identification of TCFA ready and do we know them? JACC Cardiovasc Imaging 4:656–658
22. Kusama I, Hibi K, Kosuge M, Sumita S, Tsukahara K, Okuda J, Ebina T, Umemura S, Kimura K (2012) Intravascular ultrasound assessment of the association between spatial orientation of ruptured coronary plaques and remodeling morphology of culprit plaques in ST-elevation acute myocardial infarction. Heart Vessels 27:541–547
23. Hallenbeck JM, Hansson GK, Becker KJ (2005) Immunology of ischemic vascular disease: plaque to attack. Trends Immunol 26:550–556
24. Calder PC (2003) N-3 polyunsaturated fatty acids and inflammation: from molecular biology to the clinic. Lipids 38:343–352
25. Calder PC (2006) n-3 polyunsaturated fatty acids, inflammation, and inflammatory diseases. Am J Clin Nutr 83:1505S–1519S
26. Kashiyama T, Ueda Y, Nemoto T, Wada M, Masumura Y, Matsuo K, Nishio M, Hirata A, Asai M, Kashiwase K, Kodama K (2011) Relationship between coronary plaque vulnerability and serum n-3/n-6 polyunsaturated fatty acid ratio. Circ J 75:2432–2438
27. Ogita M, Miyauchi K, Miyazaki T, Naito R, Konishi H, Tsuboi S, Dohi T, Kasai T, Yokoyama T, Okazaki S, Kurata T, Daida H (2013) Low high-density lipoprotein cholesterol is a residual risk factor associated with long-term clinical outcomes in diabetic patients with stable coronary artery disease who achieve optimal control of low-density lipoprotein cholesterol. Heart Vessels. doi:10.1007/s00380-011-0205-6
28. Kurisu S, Ishibashi K, Kato Y, Mitsuba N, Dohi Y, Nishioka K, Kihara Y (2013) Effects of lipid-lowering therapy with strong statin on serum polyunsaturated fatty acid levels in patients with coronary artery disease. Heart Vessels 28:34–38

Heart Vessels (2014) 29:638–644
DOI 10.1007/s00380-013-0408-0

ORIGINAL ARTICLE

The strain pattern, and not Sokolow–Lyon electrocardiographic voltage criteria, is independently associated with anatomic left ventricular hypertrophy

Shoichi Ehara · Takao Hasegawa · Kenji Matsumoto · Kenichiro Otsuka · Takanori Yamazaki · Tomokazu Iguchi · Yasukatsu Izumi · Kenei Shimada · Minoru Yoshiyama

Received: 2 May 2013 / Accepted: 30 August 2013 / Published online: 19 September 2013
© Springer Japan 2013

Abstract Although obesity and chest-wall thickness influence the Sokolow–Lyon electrocardiographic (ECG) voltage criteria and strain pattern, these factors have not been taken into account in previous studies that evaluate the relationship between the ECG criteria and anatomic left ventricular hypertrophy (LVH). The introduction of multislice computed tomography (MSCT) has enabled assessment of not only coronary artery stenoses but also left ventricular volume and mass, left atrial volume, and chest-wall thickness. We hypothesized that evaluating the relation between the ECG voltage criteria or strain pattern and the aforementioned factors using MSCT would be highly valuable. The study population consisted of 93 patients who required MSCT angiography. The Sokolow–Lyon voltage and strain patterns were determined to detect anatomic LVH, which was defined as increased left ventricular mass. The Sokolow–Lyon voltage criteria, as an indicator of anatomic LVH, had a sensitivity of 57 %, specificity of 67 %, positive predictive value of 36 %, and negative predictive value of 82 %. By contrast, the strain pattern had a sensitivity of 65 %, specificity of 87 %, positive predictive value of 63 %, and negative predictive value of 88 %. Multivariate analysis revealed that the strain pattern was associated with the presence of anatomic LVH, whereas the Sokolow–Lyon voltage was not. This MSCT study demonstrated that even after removing the effects of various factors, the strain pattern remained associated with the presence of anatomic LVH, in contrast to the Sokolow–Lyon voltage.

Keywords Electrocardiography · Sokolow–Lyon · Strain · Computed tomography · Hypertrophy

S. Ehara (✉) · T. Hasegawa · K. Matsumoto · K. Otsuka · T. Yamazaki · T. Iguchi · K. Shimada · M. Yoshiyama
Department of Cardiovascular Medicine, Osaka City University Graduate School of Medicine, 1-4-3 Asahi-machi, Abeno-ku, Osaka 545-8585, Japan
e-mail: ehara@med.osaka-cu.ac.jp

Y. Izumi
Department of Pharmacology, Osaka City University Graduate School of Medicine, Osaka, Japan

Introduction

The Framingham Study showed that increased left ventricular (LV) mass is associated with significantly increased cardiovascular mortality and morbidity [1]. Although newer diagnostic tools are available, left ventricular hypertrophy (LVH) detected by 12-lead electrocardiography (ECG) is a common manifestation of preclinical cardiovascular disease [2]. However, the standard Sokolow–Lyon ECG voltage criteria have low sensitivity for the detection of anatomic LVH, defined as increased LV mass [3]. In addition to the voltage criteria, the classic strain pattern of ST-segment depression and T-wave inversion in the lateral precordial leads on resting ECG is a well-known marker of the presence of anatomic LVH, which is associated with a poor prognosis in a variety of clinical populations [4, 5]. Although the strain pattern can also reflect the presence of coronary artery stenosis, the strong association between the strain pattern on ECG and increased LV mass appears to be independent of the presence of coronary artery disease [2].

Although obesity, chest-wall thickness, and the distance from the heart to the body surface influence the ECG voltage criteria or strain pattern, these factors have not been taken into account in previous studies evaluating the relationship between the ECG criteria and anatomic LVH

[2–6]. Recently, multislice computed tomography (MSCT) has reached a high spatial and temporal resolution sufficient to assess not only coronary artery stenoses and plaques but also LV function, volume, and mass, as well as left atrial (LA) volume [7–11]. Moreover, MSCT enables the measurement of the exact distance from the heart to the body surface [12, 13].

To date, little objective evidence exists regarding the relation between the ECG voltage criteria or strain pattern and numerous factors, including LV volume and mass, LA volume, chest-wall thickness, and the distance from the heart to the chest surface. Therefore, the present study was designed to evaluate this relationship using MSCT.

Patients and methods

Patients

The study was based on a retrospective analysis of data obtained from 93 consecutive patients without contraindications to MSCT such as severe renal dysfunction or iodine contrast allergy, who had a clinical indication for MSCT angiography for coronary artery evaluation. All patients underwent contrast-enhanced MSCT in the retrospective ECG-gated scanning mode and a resting 12-lead ECG. Patients with atrial fibrillation, bundle branch block, significant coronary artery stenoses with a lumen reduction of 50 % or more detected by MSCT, and history of myocardial infarction, previous coronary artery bypass grafting, or percutaneous transluminal intervention were excluded. Patients were classified into either the anatomic or nonanatomic LVH groups according to the LV mass index, measured using MSCT, as follows: anatomic LVH was diagnosed if the LV mass index was >104 g/m^2 in women or >116 g/m^2 in men; nonanatomic LVH was diagnosed if the LV mass index was ≤104 g/m^2 in women or ≤116 g/m^2 in men [2, 6, 12, 13].

The following data were collected: age, sex, presence of risk factors (smoking and hypertension, as defined by the Joint National Committee VII; diabetes mellitus, as defined by the World Health Organization Study Group; or hypercholesterolemia, as defined by the Japan Atherosclerosis Society Guidelines), body mass index (BMI), and blood pressure before image acquisition. BMI was calculated by dividing the body weight (kg) by the square of the height (m), and overweight was defined as a BMI of ≥25.0 kg/m^2. Informed consent was obtained from all patients before the study.

Electrocardiography

All resting 12-lead ECGs were obtained within 3 days before MSCT. No patients experienced chest pain during the ECG recordings. Standard amplifications, filter settings, and paper speed were used. ECGs were interpreted by two experienced readers (K.M. and T.I.) who were blinded to the clinical information. The standard Sokolow–Lyon voltage criteria for the detection of LVH were examined ($S_{V1} + R_{V5 \text{ or } V6} \geq 3.5$ mV) manually. Furthermore, repolarization abnormalities in leads V_5 and/or V_6 indicated a typical strain pattern when there was a downsloping convex ST segment with an inverted asymmetric T-wave opposite to the QRS axis [2, 4, 14].

MSCT image acquisition

The patients were scanned in the supine position, during a single breath-hold, using a 64-slice CT scanner (Somatom Sensation 64; Siemens Medical Solutions, Erlangen, Germany). Patients with a heart rate of >65 beats/min received 20–60 mg metoprolol orally 2 h before the MSCT scan. In addition, all patients received 0.6 mg nitroglycerin sublingually immediately before MSCT.

For coronary CT angiography, 65–85 ml of contrast medium (Iopamiron 370; Bayer Health Care, Berlin, Germany) was injected into the cubital vein through a dual-head injector at a rate of 3.5–4.0 ml/s, depending on the body weight; thereafter, 30 ml of a saline solution chaser was injected. The scan delay was determined using the bolus tracking technique. The CT examination was performed with a tube voltage of 120 kV, effective tube current–time product of 770 effective mAs, collimation of 64 × 0.6 mm, pitch of 0.2, and gantry rotation time of 330 ms.

CT image analysis

CT image analysis was performed by a single experienced cardiologist (K.O.) who was blinded to the clinical information and ECG findings. The MSCT evaluation factors are shown in Fig. 1. First, for evaluation of coronary artery stenosis, ECG-correlated image reconstruction was retrospectively performed using an effective slice thickness of

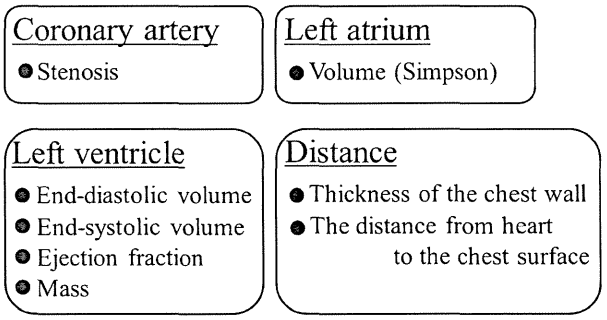

Fig. 1 Multislice computed tomography evaluation factors